Supplement of Atmos. Meas. Tech., 14, 309–334, 2021
https://doi.org/10.5194/amt-14-309-2021-supplement

Atmospheric Measurement Techniques
Open Access
EGU

Supplement of

ModIs Dust AeroSol (MIDAS): a global fine-resolution dust optical depth data set

Antonis Gkikas et al.

Correspondence to: Antonis Gkikas (agkikas@noa.gr)

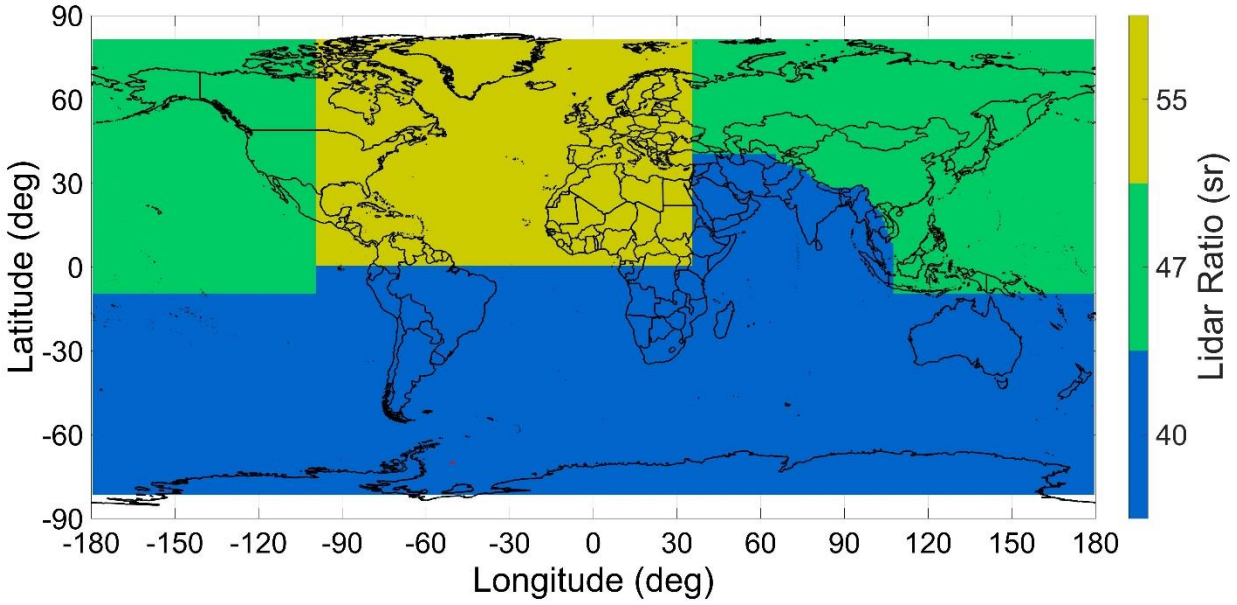

Figure S1: Global geographical distribution of dust lidar ratios considered in the LIVAS pure dust product.

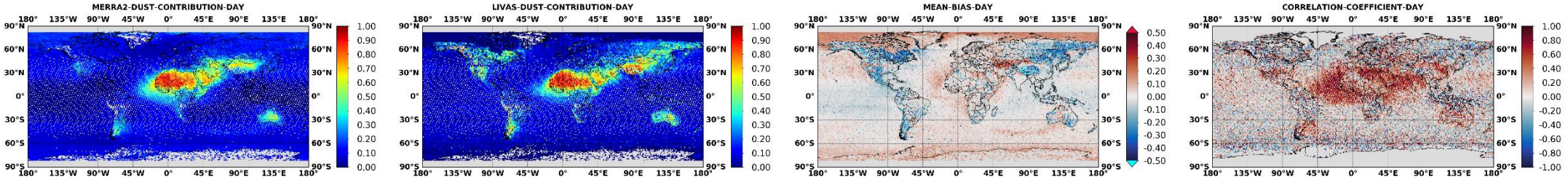

(i-a) (i-b) (i-c) (i-d)

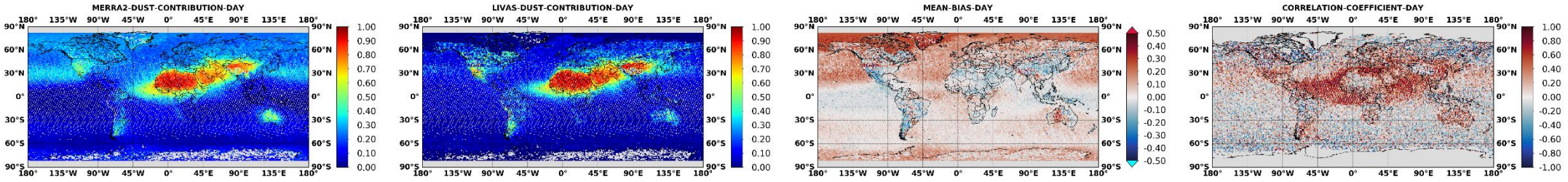

(ii-a) (ii-b) (ii-c) (ii-d)

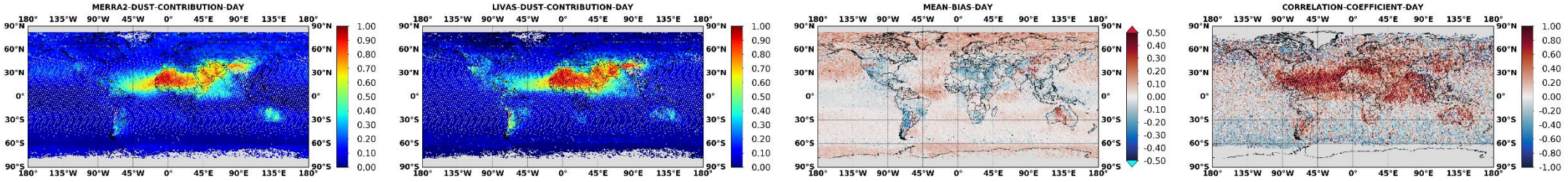

(iii-a) (iii-b) (iii-c) (iii-d)

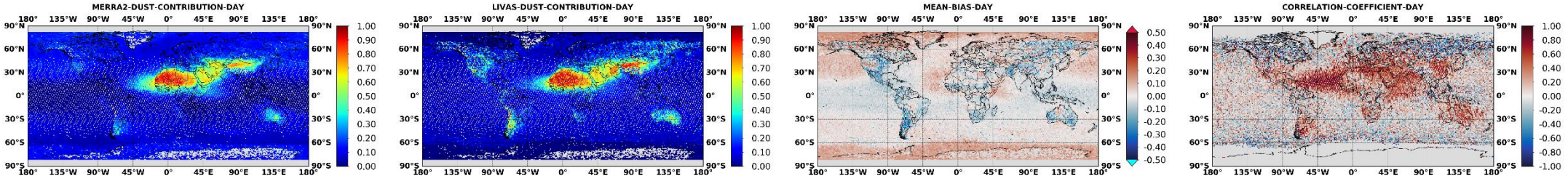

(iv-a) (iv-b) (iv-c) (iv-d)

Figure S2: Geographical distributions of: (a) the MERRA-2 dust contribution, (b) the LIVAS dust contribution, (c) the mean bias defined as MERRA2 – LIVAS and (d) the correlation coefficient. The obtained results, at 1° x 1° spatial resolution, are given separately for: (i) December-January-February (DJF), (ii) March-April-May (MAM), (iii) June-July-August (JJA) and (iv) September-October-November (SON), during the period 2007 – 2015.

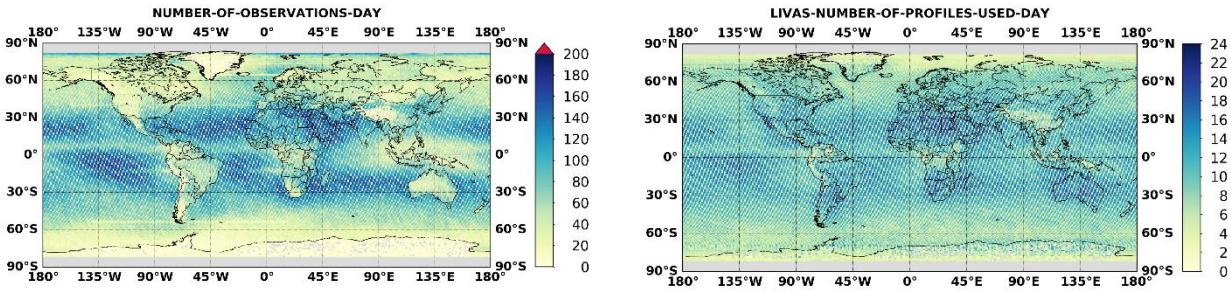

(i) **(ii)**

Figure S3: Global geographical distributions of the: **(i)** number of days with available LIVAS data during the period 2007 – 2015 and **(ii)** average number of CALIOP L2 profiles aggregated for the derivation of the 1° x 1° LIVAS grid cell.

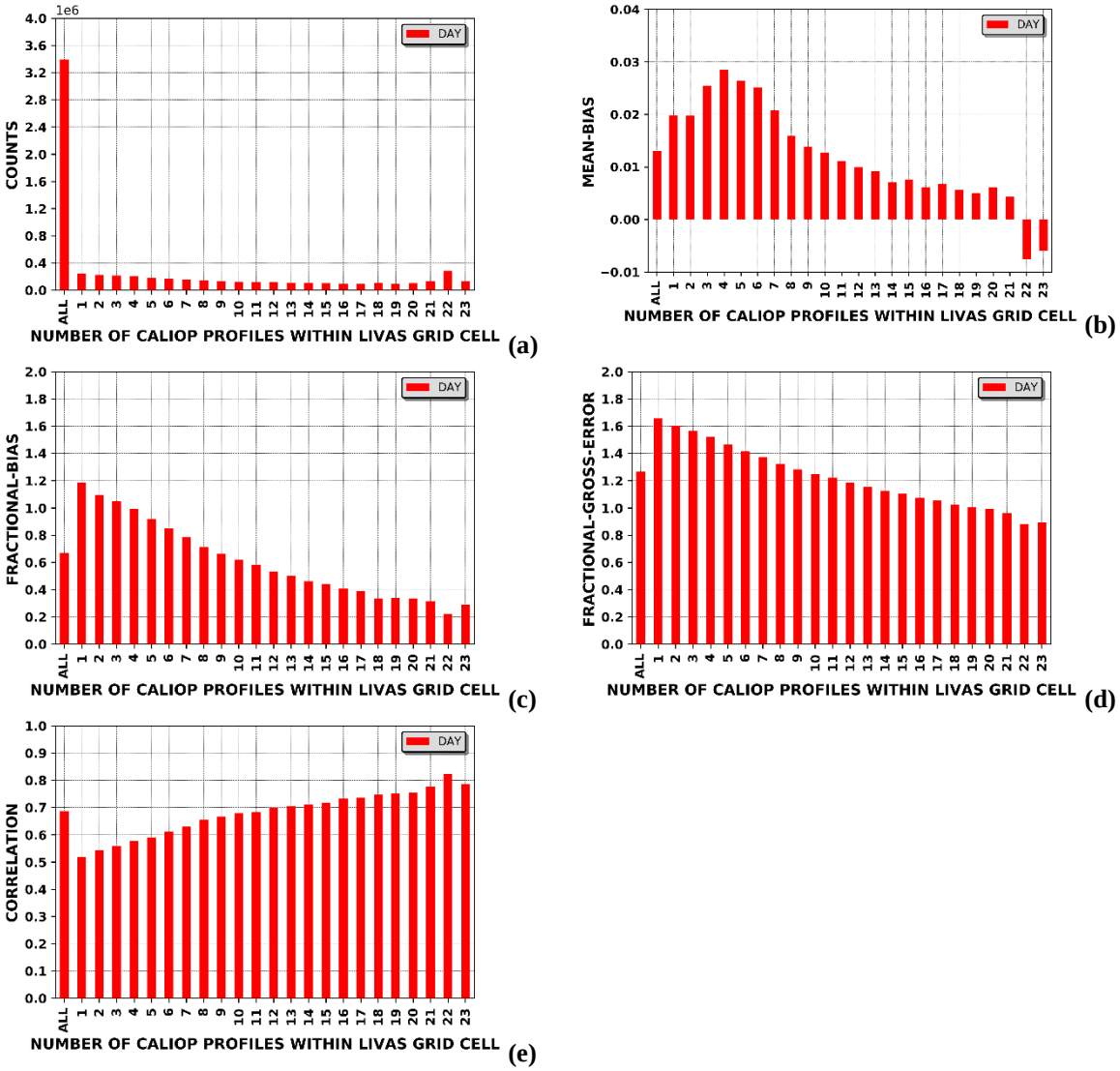

(a) **(b)** **(c)** **(d)** **(e)**

Figure S4: Histograms of the: **(a)** number of LIVAS-MERRA-2 collocated pairs, **(b)** mean bias, **(c)** fractional bias, **(d)** fractional gross error and **(e)** correlation coefficient calculated between MERRA-2 and LIVAS dust fractions, for daytime conditions and at global scale over the period 2007 – 2015, for individual bins of CALIOP number of profiles residing within the 1° x 1° LIVAS grid cell.

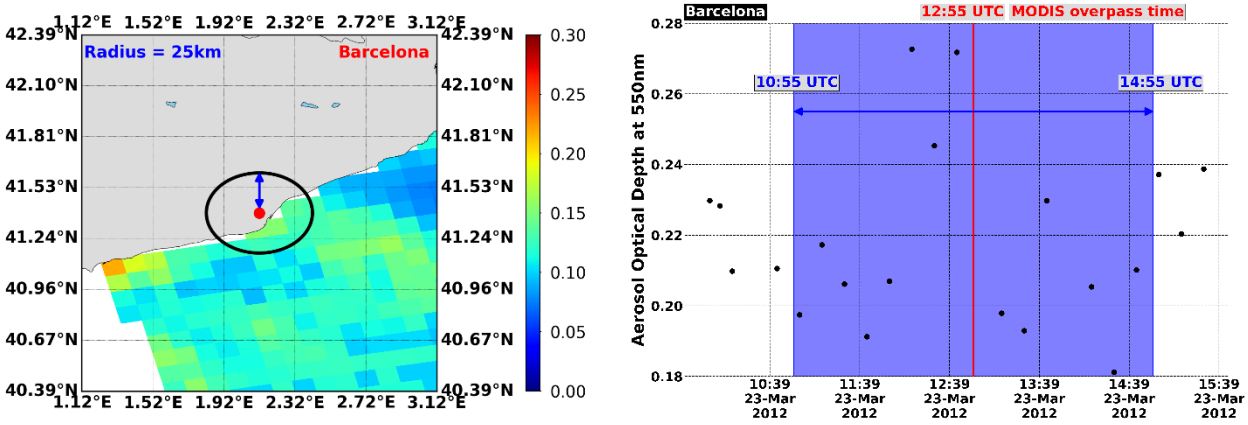

Figure S5: A schematic paradigm of the applied methodology for the collocation between MODIS L2 observations and AERONET almucantar retrievals. (**i**) The satellite AODs are spatially averaged, when at least one of them resides within the circle area (black curve), centered over an AERONET station (red dot), with a radius of 25 km (blue double-side arrow). (**ii**) The ground-based AODs (black circles) are temporally averaged when at least one of them falls within the time-window of 4 hours (blue shaded area) centered over the satellite overpass time (red thick line).

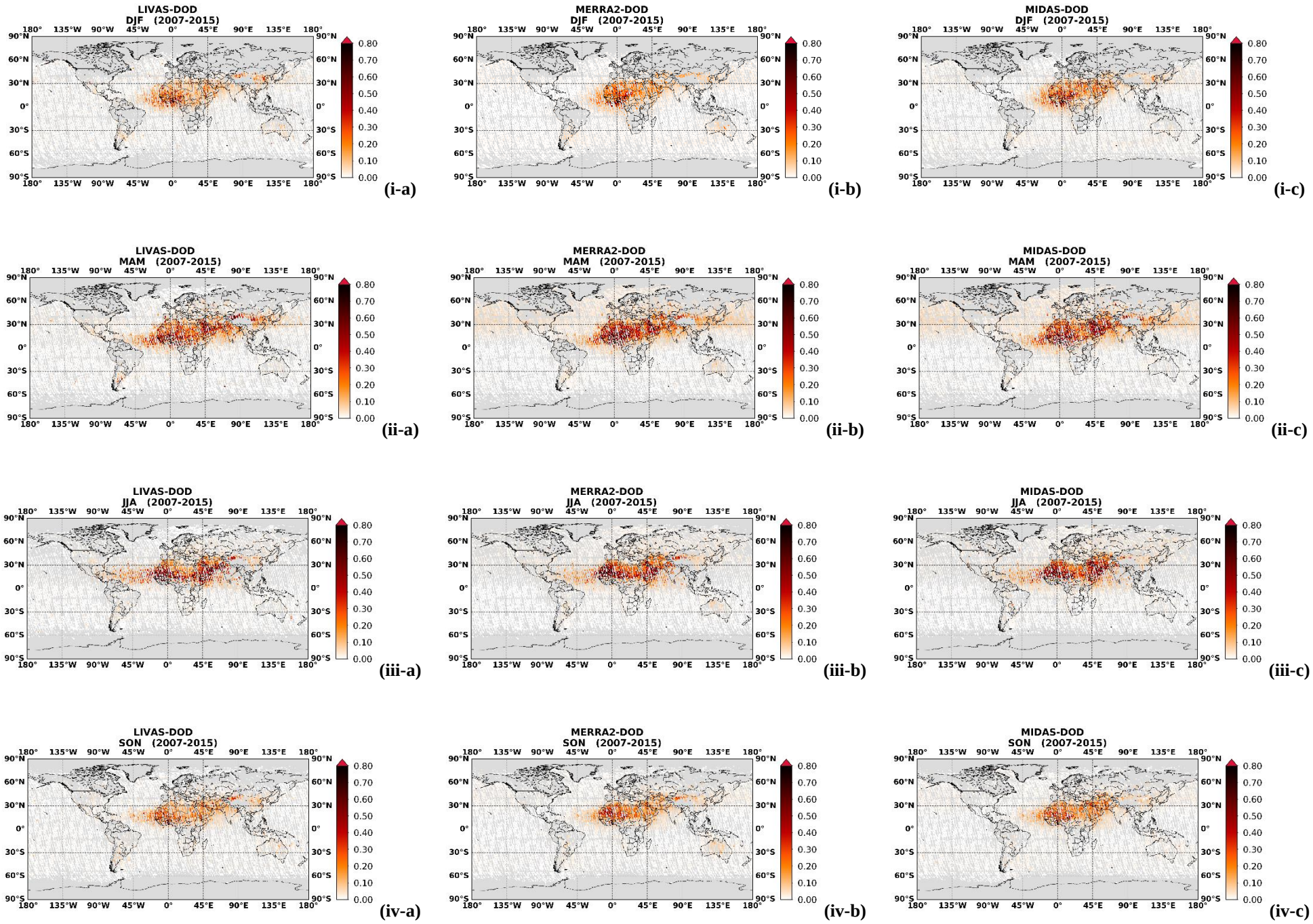

Figure S6: Seasonal geographical collocated distributions at 1° x 1° spatial resolution of daytime: **(a)** LIVAS DOD_{532nm}, **(b)** MERRA-2 DOD_{550nm} and **(c)** MIDAS DOD_{550nm}. The average maps, representative for the period 2007 – 2015, are presented separately for: **(i)** DJF, **(ii)** MAM, **(iii)** JJA and **(iv)** SON.

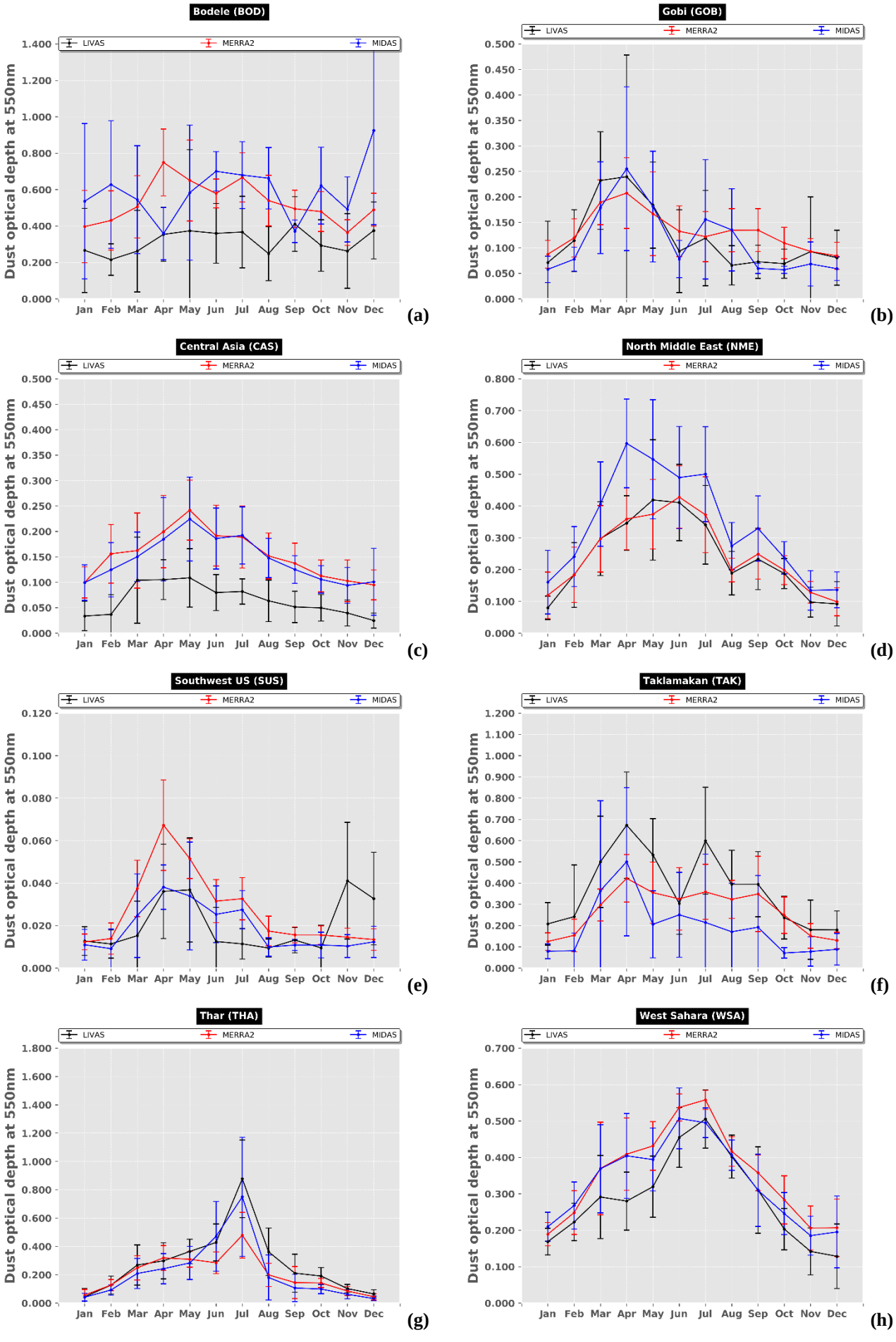
Bodele (BOD)
LIVAS
MERRA2
MIDAS
Dust optical depth at 550nm
Jan Feb Mar Apr May Jun Jul Aug Sep Oct Nov Dec
(a)
Gobi (GOB)
(b)
Central Asia (CAS)
(c)
North Middle East (NME)
(d)
Southwest US (SUS)
(e)
Taklamakan (TAK)
(f)
Thar (THA)
(g)
West Sahara (WSA)
(h)

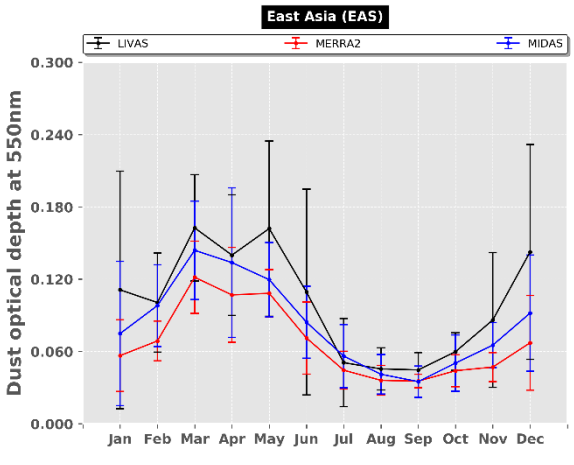
East Asia (EAS)
LIVAS
MERRA2
MIDAS
Dust optical depth at 550nm
0.300
0.240
0.180
0.120
0.060
0.000
Jan Feb Mar Apr May Jun Jul Aug Sep Oct Nov Dec

(i)

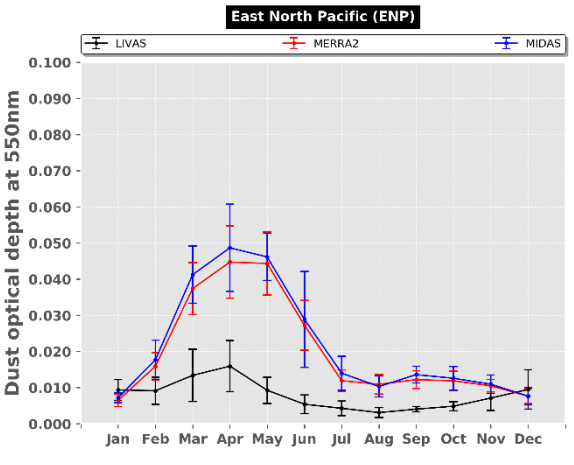
East North Pacific (ENP)
LIVAS
MERRA2
MIDAS
Dust optical depth at 550nm
0.100
0.090
0.080
0.070
0.060
0.050
0.040
0.030
0.020
0.010
0.000
Jan Feb Mar Apr May Jun Jul Aug Sep Oct Nov Dec

(j)

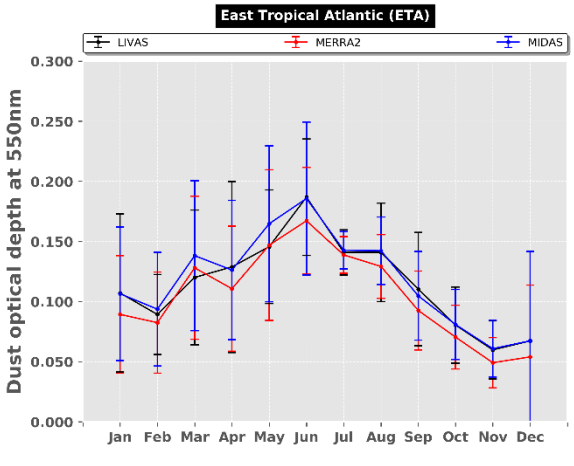
East Tropical Atlantic (ETA)
LIVAS
MERRA2
MIDAS
Dust optical depth at 550nm
0.300
0.250
0.200
0.150
0.100
0.050
0.000
Jan Feb Mar Apr May Jun Jul Aug Sep Oct Nov Dec

(k)

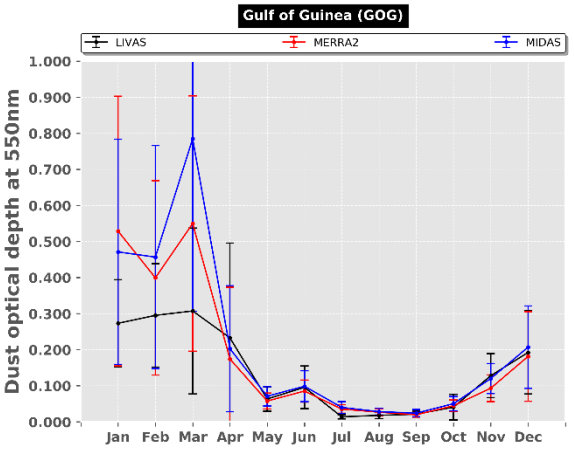
Gulf of Guinea (GOG)
LIVAS
MERRA2
MIDAS
Dust optical depth at 550nm
1.000
0.900
0.800
0.700
0.600
0.500
0.400
0.300
0.200
0.100
0.000
Jan Feb Mar Apr May Jun Jul Aug Sep Oct Nov Dec

(l)

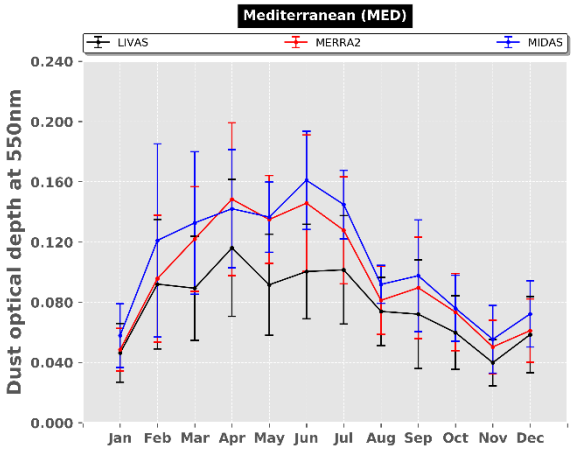
Mediterranean (MED)
LIVAS
MERRA2
MIDAS
Dust optical depth at 550nm
0.240
0.200
0.160
0.120
0.080
0.040
0.000
Jan Feb Mar Apr May Jun Jul Aug Sep Oct Nov Dec

(m)

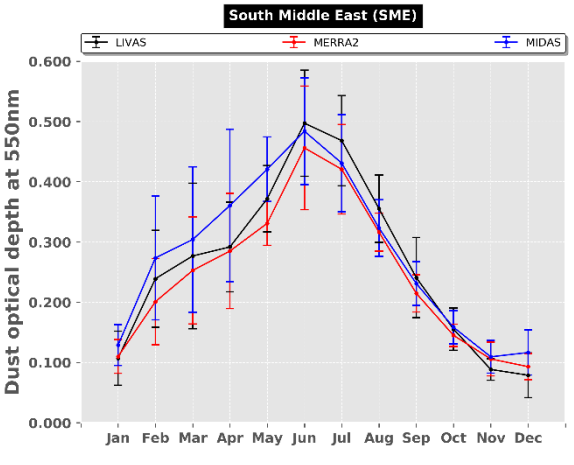
South Middle East (SME)
LIVAS
MERRA2
MIDAS
Dust optical depth at 550nm
0.600
0.500
0.400
0.300
0.200
0.100
0.000
Jan Feb Mar Apr May Jun Jul Aug Sep Oct Nov Dec

(n)

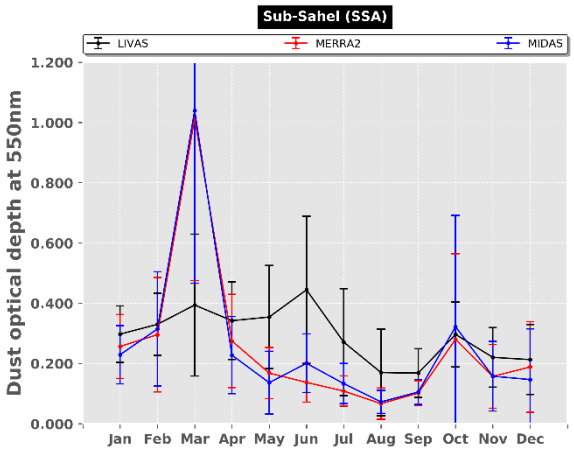
Sub-Sahel (SSA)
LIVAS
MERRA2
MIDAS
Dust optical depth at 550nm
1.200
1.000
0.800
0.600
0.400
0.200
0.000
Jan Feb Mar Apr May Jun Jul Aug Sep Oct Nov Dec

(o)

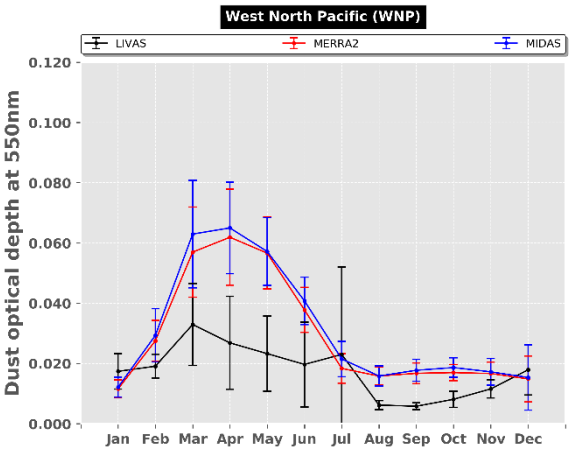
West North Pacific (WNP)
LIVAS
MERRA2
MIDAS
Dust optical depth at 550nm
0.120
0.100
0.080
0.060
0.040
0.020
0.000
Jan Feb Mar Apr May Jun Jul Aug Sep Oct Nov Dec

(p)

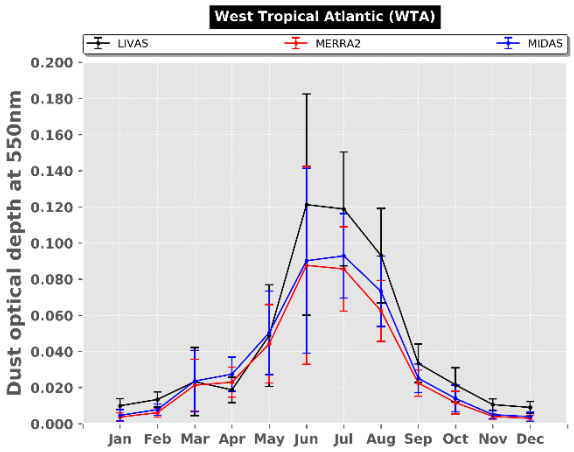

(q)

Figure S7: Intra-annual variability of collocated LIVAS (black curve), MERRA-2 (red curve) and MIDAS (blue curve) monthly DODs regionally averaged over the: **(a)** Bodélé Depression (BOD), **(b)** Gobi Desert (GOB), **(c)** Central Asia (CAS), **(d)** North Middle East (NME), **(e)** southwest United States (SUS), **(f)** Taklamakan Desert (TAK), **(g)** Thar Desert (THA), **(h)** West Sahara (WSA), **(i)** East Asia (EAS), **(j)** East North Pacific (ENP), **(k)** East Tropical Atlantic (ETA), **(l)** Gulf of Guinea (GOG), **(m)** Mediterranean (MED), **(n)** South Middle East (SME), **(o)** Sub-Sahel (SSA), **(p)** West North Pacific (WNP) and **(q)** West Tropical Atlantic (WTA). The error bars correspond to the standard deviation computed from the interannual timeseries during the period 2007 – 2015.

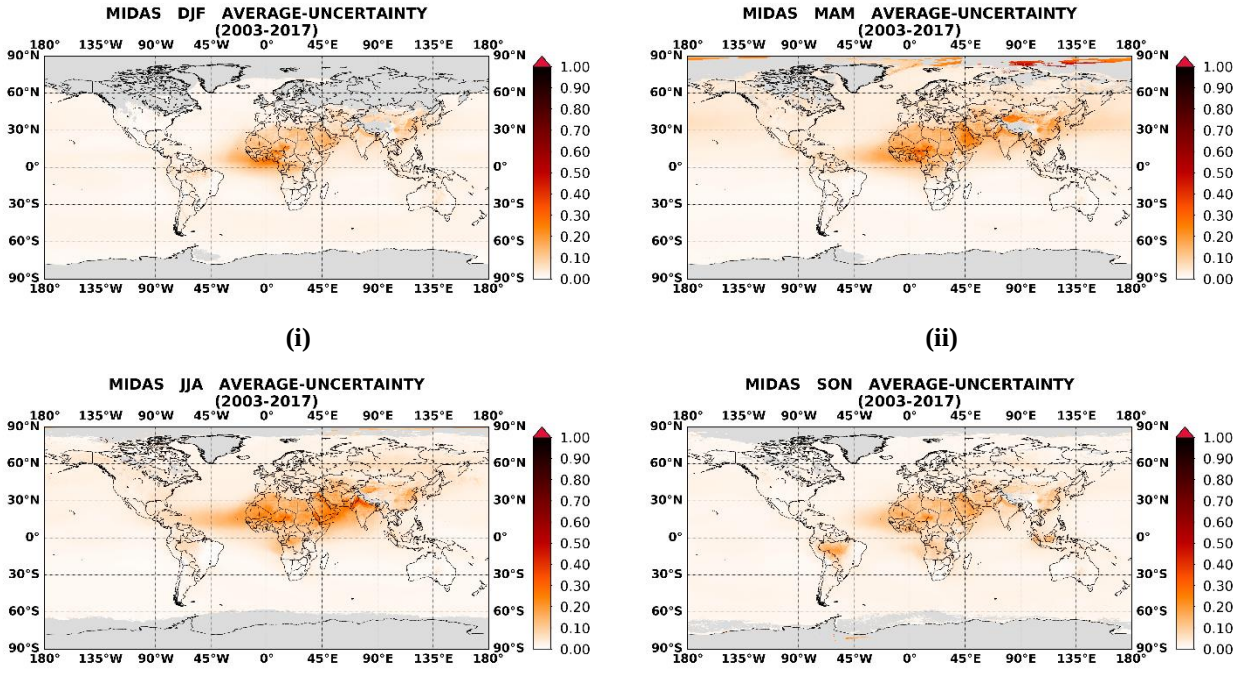

(i) **(ii)**

(iii) **(iv)**

Figure S8: Seasonal geographical distributions of the average daily DOD uncertainty for: **(i)** December-January-February (DJF), **(ii)** March-April-May (MAM), **(iii)** June-July-August (JJA) and **(iv)** September-October-November (SON) over the period 2003 – 2017.